

CFD ANALYSIS OF HYDROGEN LEAKAGE FROM A SMALL HOLE IN A SLOPING ROOF HYDROGEN REFUELING STATION

Weiye Cui^{1,2,3}, Liang Tong^{1,2,4}, Yupeng Yuan^{1,2,4,5} and Chengqing Yuan^{1,2,4,5}

¹ State Key Laboratory of Maritime Technology and Safety, Wuhan University of Technology, Wuhan, 430063, China.

² National Engineering Research Center for Water Transport Safety, Wuhan University of Technology, Wuhan, 430063, China.

³ School of Naval Architecture, Ocean and Energy Power Engineering, Wuhan University of Technology, Wuhan, 430063, China

⁴ Reliability Engineering Institute, School of Transportation and Logistics Engineering, Wuhan University of Technology, Wuhan, 430063, China, ypyuan@whut.edu.cn

⁵ Academician Workstation of COSCO SHIPPING Group, Shanghai, 200135, China

ABSTRACT

As a key link in the application of hydrogen energy, hydrogen refueling stations are significant for their safe operation. This paper established a three-dimensional 1:1 model for a seaport hydrogen refueling station in Ningbo City. In this work, the CFD software FLUENT was used to study the influence of leakage angles on the leakage of high-pressure hydrogen through a small hole. Considering the calculation accuracy and efficiency, this paper adopted the pseudo-diameter model. When the obstacle was far from the leakage hole, it had almost no obstructive effect on the jet's main body. Still, it affected the hydrogen, whose momentum in the outer layer of the jet has been significantly decayed. In this condition, there would be more hydrogen in stagnation. Thus the volume of the flammable hydrogen cloud was hardly affected, while there was a significant increase in the volume of the hazardous hydrogen cloud. When the obstacle was close to the leakage hole, it directly affected the jet's main body. Therefore the volume of the flammable hydrogen cloud increased. However, the air impeded the hydrogen jet relatively less because the hydrogen jet contacted the obstacle more quickly. The hydrogen jet blocked by the obstacle still has some momentum. Therefore, there was no more hydrogen in stagnation and no significant increase in the volume of the hazardous hydrogen cloud.

NOMENCLATURE

A	outlet area (m^2)
C_0	leakage coefficient
C_1	empirical coefficient
C_{1e}	model constant
C_2	model constant
C_{3e}	coefficient characterizing the angle between the flow direction and the gravity direction
c_p	constant pressure specific heat capacity ($\text{J}/(\text{kg}\cdot\text{K})$)
d	outlet diameter (m)
E	total energy of the gas (J)
f	force per unit mass (N)
G	turbulent energy (J)
J	diffusion coefficient
k	heat transfer coefficient
p	pressure (Pa)
Pr_t	turbulent Prandtl number
Q	leakage mass flow rate (kg/s)
R	gas constant ($\text{J}/(\text{kg}\cdot\text{K})$)
S	source terms
t	time (s)
T	temperature (K)

T_{ij}	partial stress tensor (N/m ²)
u	velocity (m/s)
w	mass fraction
x	distance in the horizontal direction (m)
Y_M	dissipation term caused by turbulent fluctuations
Greek	
ρ	density (kg/m ³)
∇	laplace operator
κ	turbulent energy (J)
ε	dissipation rate
σ_κ	Prandtl number of the κ equation
σ_ε	Prandtl number of the ε equation
μ	kg/(m·s)
θ	angle between the jet centerline and horizontal (°)
γ	gas specific heat ratio
Subscripts	
0	leakage source
1	actual outlet
2	equivalent outlet
b	buoyancy
e	nozzle outlet
eff	effective value
gas	jet gas
j	direction in the three-dimensional Cartesian coordinate system
k	velocity gradient
i	direction in the three-dimensional Cartesian coordinate system
n	component n
ps	pseudo-diameter
s	component s
t	turbulent
∞	atmospheric

1.0 INTRODUCTION

With the development of carbon-neutral policies such as the Paris Agreement, hydrogen energy, as a zero-carbon renewable energy source, is gradually becoming an essential player in the global energy transition [1]. Hydrogen refueling stations are necessary infrastructure for supplying hydrogen to end-use hydrogen equipment, and their safe operation is of great significance. Hydrogen is the gas with the smallest molecular weight in nature, which has the characteristics of being flammable and explosive [2], having a wide combustion limit [3], and having low minimum ignition energy [4]. Hydrogen refueling station equipment has many joints and valves, which are prone to hydrogen leakage caused by poor sealing [5][6].

This work analyzed the effect of three different leakage angles on hydrogen leakage diffusion at a seaport hydrogen refueling station in Ningbo City. The pseudo-diameter model proposed by Birch et al. [7] in 1987 was used to balance calculation accuracy and efficiency. This model simplifies the generation of a series of complex shock structure when high-pressure hydrogen leakage from a small hole to the outside by assuming an equivalent outlet. The model's accuracy in this paper was verified by comparing it with the simulation of Li et al. [8] and the experimental data of Han et al. [9]. The effect of grid number was excluded by grid-independent verification. The CFD code was used to analyze the danger of hydrogen leakage and the location where hydrogen tends to accumulate under different conditions. Based on the simulation results, the targeted arrangement of hydrogen detectors can reduce the risk caused by hydrogen leakage by providing timely alarms after hydrogen leakage.

2.0 THEORETICAL MODEL

2.1 Control equations

Mixing hydrogen with air satisfies the mass conservation, momentum, and energy conservation equations, and also follows the law of conservation of components. The leakage and diffusion process satisfies the following control equations.

Mass conservation equation:

$$\frac{\partial \rho}{\partial t} + \frac{\partial}{\partial x_i} (\rho u_i) = 0 \quad (1)$$

where ρ – density, kg/m³; t – time, s; x_i – distance in the horizontal direction, m; u_i – velocity in direction i , m/s.

Momentum equation:

$$\frac{\partial}{\partial t} (\rho u_i) + \frac{\partial}{\partial x_i} (\rho u_i u_j) = -\frac{\partial p}{\partial x_i} + \frac{\partial T_{ij}}{\partial x_i} + \rho f_i \quad (2)$$

where u_j – velocity in direction j , m/s; p – pressure, Pa; T_{ij} – partial stress tensor, where i denotes the normal direction of the plane of action of the partial stress tensor, j denotes the direction of projection of the stress component, N/m²; f_i – force per unit mass in the direction i , N.

Energy equation:

$$\frac{\partial}{\partial t} (\rho E) + \frac{\partial}{\partial x_i} [u_i (\rho E + p)] = \frac{\partial}{\partial x_j} \left[\left(k_{\text{eff}} + \frac{c_p \mu_t}{Pr_t} \right) \frac{\partial T}{\partial x_j} + u_i (T_{ij})_{\text{eff}} \right] \quad (3)$$

where E – total energy of the gas, J; x_j – distance in the horizontal direction, m; k_{eff} – effective heat transfer coefficient; c_p – constant pressure specific heat capacity, J/(kg·K); μ_t – turbulent viscosity, kg/(m·s); Pr_t – turbulent Prandtl number, set as 1; $(T_{ij})_{\text{eff}}$ – effective partial stress tensor, N/m².

Transport equation:

$$\frac{\partial}{\partial t} (\rho w_n) + \nabla \cdot (\rho \mathbf{u} w_n) = -\nabla \cdot \mathbf{J}_s \quad (4)$$

where w_n – mass fraction of component n ; ∇ – Laplace operator; \mathbf{u} – velocity vector, m/s; \mathbf{J}_s – diffusion coefficient of component s .

Turbulence model:

When high-pressure hydrogen leaks, there is an enormous pressure difference between the inside and outside. At the same time, the hydrogen leakage diffusion is obstructed by buildings and so on. Hence, the flow is very complex and belongs to typical turbulent flow, so the realizable κ - ε turbulence model is chosen in this paper.

The turbulent kinetic energy κ equation:

$$\frac{\partial (\rho \kappa)}{\partial t} + \frac{\partial (\rho \kappa u_j)}{\partial x_j} = \frac{\partial}{\partial x_j} \left[\left(\mu + \frac{\mu_t}{\sigma_\kappa} \right) \frac{\partial \kappa}{\partial x_j} \right] + G_\kappa + G_b + S_\kappa - \rho \varepsilon - Y_M \quad (5)$$

Dissipation rate ε equation:

$$\frac{\partial (\rho \varepsilon)}{\partial t} + \frac{\partial (\rho \varepsilon u_i)}{\partial x_i} = \frac{\partial}{\partial x_j} \left[\left(\mu + \frac{\mu_t}{\sigma_\varepsilon} \right) \frac{\partial \varepsilon}{\partial x_j} \right] + \rho C_1 E \varepsilon - \rho C_2 \frac{\varepsilon^2}{\kappa + \sqrt{\nu \varepsilon}} + C_{1\varepsilon} \frac{\varepsilon}{\kappa} C_{3\varepsilon} G_b + S_\varepsilon \quad (6)$$

where κ – turbulent energy, J; ε – dissipation rate; σ_κ – Prandtl number of the κ equation, set as 1.0; σ_ε – Prandtl number of the ε equation, set as 1.2; μ – fluid viscosity, kg/(m·s); G_k – turbulent energy caused by the velocity gradient, J; G_b – turbulent energy caused by buoyancy, J; $C_{1\varepsilon}$ – model constant, set as 1.44; C_2 – model constant, set as 1.90; C_1 – empirical coefficient; $C_{3\varepsilon}$ – coefficient characterizing the angle between the flow direction and the gravity direction; Y_M – dissipation term caused by turbulent fluctuations; S_k and S_ε – source terms.

Pseudo-diameter model:

High-pressure underexpanded gas leaks can produce complex shock structures such as Mach disks, which require complex grids and consume many resources if predicted accurately. Since this paper is more concerned with the diffusion of hydrogen leakage at larger scales than the region near the leakage hole, a pseudo-diameter model was used to simplify the leakage process. There are various existing pseudo-diameter models, and Birch et al. [7][10], Ewan and Moodie [11], Yuceil and Otugen [12], Schefer et al. [13] and Molkov et al. [14] have proposed corresponding pseudo-diameter models. After verification by Li et al. [8], the model proposed by Birch in 1987 was the closest to the actual situation, so the Birch 1987 pseudo-diameter model was used in this paper, as shown in Figure 1. In the Birch 1987 Pseudo-diameter model, an equivalent outlet is assumed, the leakage gas is pure hydrogen, and the leakage flow rate is equal to the actual flow rate. The gas leakage process follows the law of conservation of momentum, and the temperature and pressure of the gas are equal to the temperature and pressure of the environment [7].

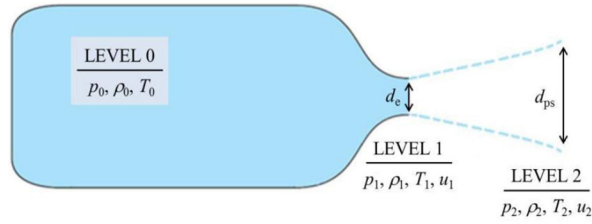


Figure 1. Pseudo-diameter model

Mass conservation equation:

$$\rho_1 u_1 A_1 = \rho_2 u_2 A_2 \quad (7)$$

in this paper:

$$A_1 = \frac{\pi d_e^2}{4} \quad (8)$$

$$A_2 = \frac{\pi d_{ps}^2}{4} \quad (9)$$

Momentum conservation equation:

$$\rho_2 u_2^2 A_2 = \rho_1 u_1^2 A_1 + (p_1 - p_2) A_1 \quad (10)$$

Pseudo diameter:

$$\frac{d_{ps}}{d_e} = \frac{\rho_1 u_1}{\sqrt{\rho_{gas}(p_1 - p_\infty + \rho_1 u_1^2)}} \quad (11)$$

where: ρ_1, ρ_2 – gas densities at the actual and equivalent outlets, kg/m³; u_1, u_2 – gas velocities at the actual and equivalent outlets, m/s; A_1, A_2 – actual outlet and equivalent outlet area, m²; d_e, d_{ps} – actual

outlet and equivalent outlet diameters, m; ρ_{gas} – density of the jet gas, kg/m^3 ; ρ_{∞} – atmospheric density, kg/m^3 .

Leakage mass flow rate:

The empirical formula for the mass flow rate of a supersonic gas is[15]:

$$Q = C_0 A_1 p_0 \sqrt{\frac{MY}{RT_1} \left(\frac{2}{\gamma+1} \right)^{\frac{\gamma+1}{\gamma-1}}} \quad (12)$$

where: Q – leakage mass flow rate, kg/s; C_0 – leakage coefficient, in this paper, the leakage hole is circular, take 1; p_0 is the leakage source pressure, Pa; M – the molar mass of hydrogen, taken as $0.002 \text{ kg} \cdot \text{mol}^{-1}$; γ – gas specific heat ratio, for hydrogen, 1.4; R – gas constant, $\text{J}/(\text{kg} \cdot \text{K})$; T_1 – the temperature at the actual outlet, K.

2.2 Hydrogen refueling station geometry model

This paper establishes a 1:1 3D model regarding an actual hydrogen refueling station in Ningbo, China. According to the accident statistics of hydrogen refueling stations, the leakage of the filling hose caused by seal failure accounts for 13.95% of the total number of accidents, second only to all kinds of joint failures [5][6]. Smaller holes have a higher probability of hydrogen leaks than catastrophic leaks with larger holes. The filling hose was therefore selected as the leak location and was assumed to have a seal failure resulting in a microporous leak. The leak hole was a circular 1 mm diameter leak hole. Therefore, this paper selects the filling hose next to the hydrogen refueling machine as the leakage point. The structural parameters of the hydrogen refueling station and the leakage location are shown in Figure 2.

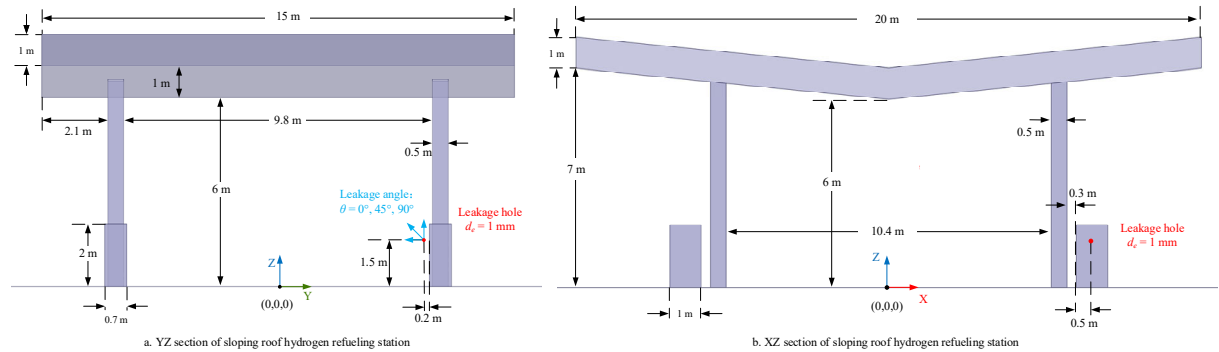


Figure 2. Hydrogen refueling station cross-section and location of leakage hole

The grid region is divided into three parts: core, stretched, and refined domains. The grid cell within the refined domain must be controlled at $A_{\text{control volume}} (\text{single grid area at the leak}) = 1.25 \cdot A_{\text{leak}}$ (leakage area) for hydrogen leaks[16]. The grids in the refined domain are uniform, and all have a grid size of 0.01 m. The grids in the core domain cover the area from the leak-side hydrogen dispenser to the contralateral hydrogen dispenser. Three grid sizes were selected for the core area (grid size=0.05 m, grid number=156983; grid size=0.10 m, grid number=292852; grid size=0.15 m, grid number=458289) to verify grid independence. Simulations were performed at the leakage angle $\theta=0^\circ$. As shown in Figure 3, the results of the two cases with grid numbers 292852 and 458289 did not differ much, while the case with grid number 156983 shows a significant deviation from the remaining two cases. In order to balance the computational accuracy and simulation efficiency, the case with grid number 292852 was used.

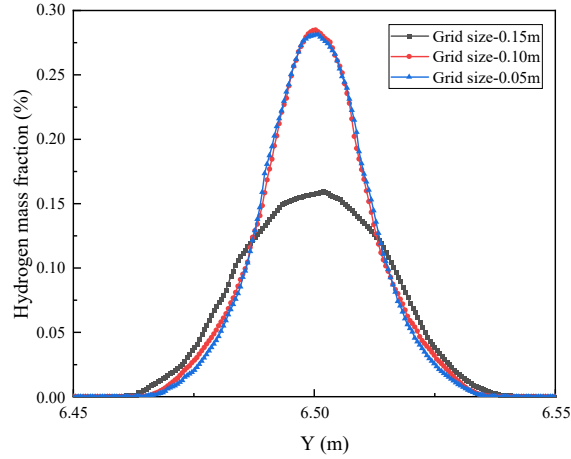


Figure 3. Grid irrelevance test on leakage angle $\theta=0^\circ$, no wind condition

A leakage case similar to that in references [8][9] was constructed to validate the pseudo-diameter and hydrogen diffusion model established in this paper. As shown in Figure 4, the simulation data in this paper agreed with the simulation data and experimental data. Therefore, it can be demonstrated that the pseudo-diameter and hydrogen leakage diffusion models constructed in this paper align with reality, and the subsequent simulation results were reliable.

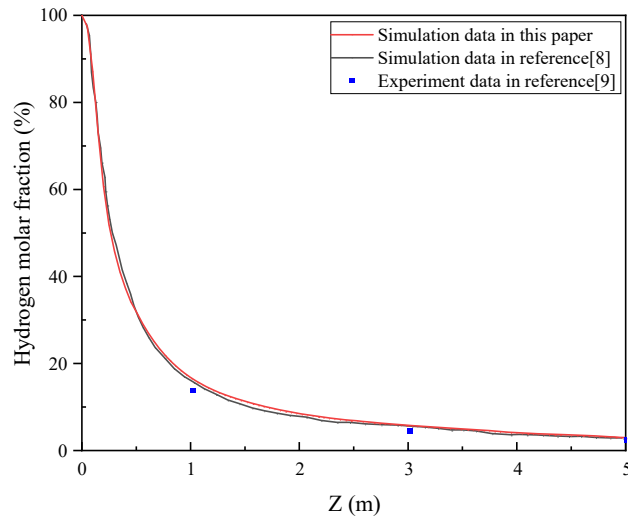


Figure 4. CFD model validation of hydrogen diffusion

2.2 Initial and boundary conditions

The boundary and initial conditions set for the CFD numerical model are as follows:

1. In the CFD model, the ground, hydrogen dispenser, columns, and roof were set as no slip walls; the leak hole was mass flow inlet; the surrounding atmosphere was pressure outlet.
2. CFD models contain only fluid domains. The initial ambient temperature of the model was 300 K, and the ambient pressure was 101 kPa; considering the influence of gravity and buoyancy on the diffusion of hydrogen leakage, the gravitational acceleration direction was vertically downward and was set as $9.81 \text{ m}\cdot\text{s}^{-2}$ to turn on the buoyancy diffusion effect.

3. The pressure was maintained at 45 MPa at all times during the leakage; the leakage hole was a 1 mm diameter circle and remained constant.

4. The leaking gas is 100% pure hydrogen at the same temperature as the external environment. Gas type set as ideal compressible gas.

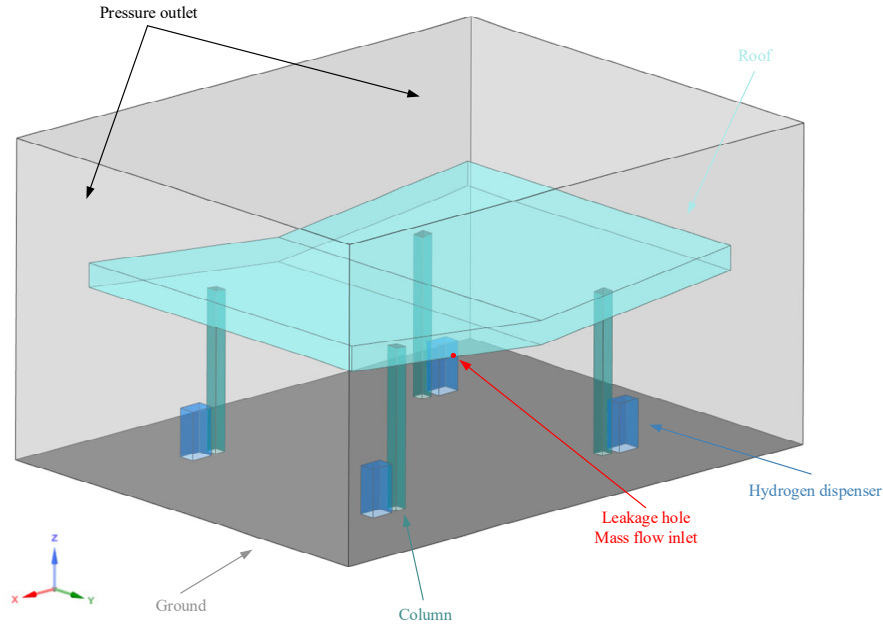


Figure 5. CFD model validation of hydrogen diffusion

3.0 RESULTS AND DISCUSSION

In order to investigate the effect of leakage angle on hydrogen leakage dispersion, simulations were carried out in this section at three different leakage angles, i.e., $\theta=0^\circ$, 45° , and 90° . To quantify the effect of different leakage angles on hydrogen diffusion, the flammable and hazardous volumes were used to quantify the risk in different leakage situations. The flammable volume was the volume of the hydrogen cloud within the flammable limit, i.e., the volume of the "hydrogen-air" mixture with a molar fraction of hydrogen between 4 and 75%. The hazardous volume was the "hydrogen-air" mixture with a molar fraction of hydrogen above 1%. Where 1% was obtained from the lower flammable limit of hydrogen $4\% \times 1/4$, which may be potentially hazardous. Hydrogen concentrations below 1% were usually considered perfectly safe and difficult to trigger a hydrogen monitoring alarm system [17].

When the leakage angle $\theta=0^\circ$, the hydrogen jet body was not affected because the opposite side hydrogen dispenser was far from the leakage hole. As shown in Figure 7 a and Figure 8 a, at $t=1$ s, the hydrogen jet body has been stabilized, and the volume of the flammable hydrogen cloud has reached the maximum value and remains constant. The momentum of the thin hydrogen (1% to 4%) in the outer layer of the hydrogen jet has dropped significantly after being hindered by the air. The momentum decreased further after being hindered by the hydrogen dispenser. Because the leakage was carried out in a no-wind condition, large amounts of hydrogen reached stagnation near the obstacle, and the volume of the hazardous hydrogen cloud kept rising. As shown in Figure 8 b, at $t=12$ s, the volumes of the hazardous hydrogen cloud reached their peak and were subsequently stable.

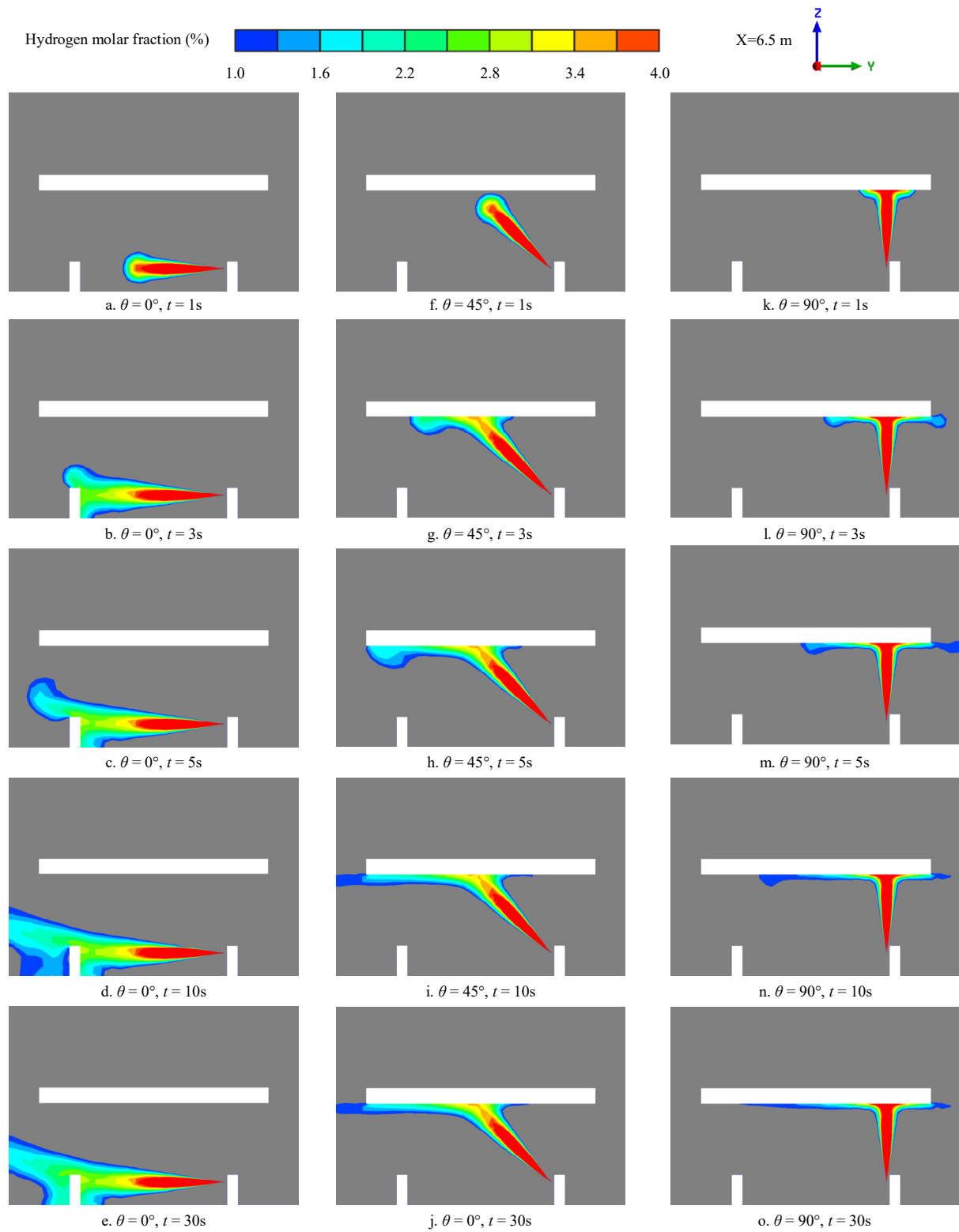


Figure 6. Hydrogen distribution in YZ section at different leakage angles

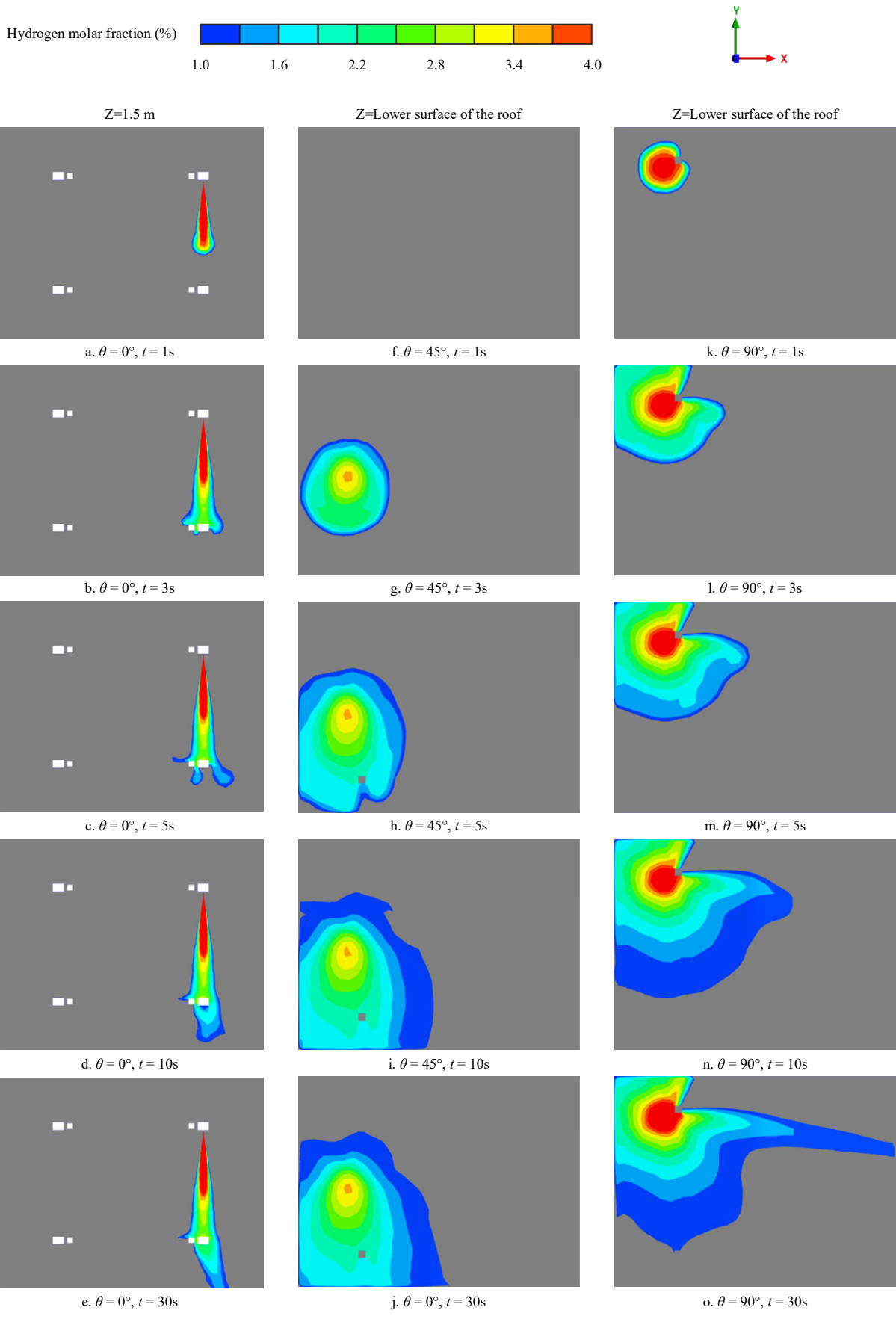


Figure 7. Hydrogen distribution in XY section at different leakage angles

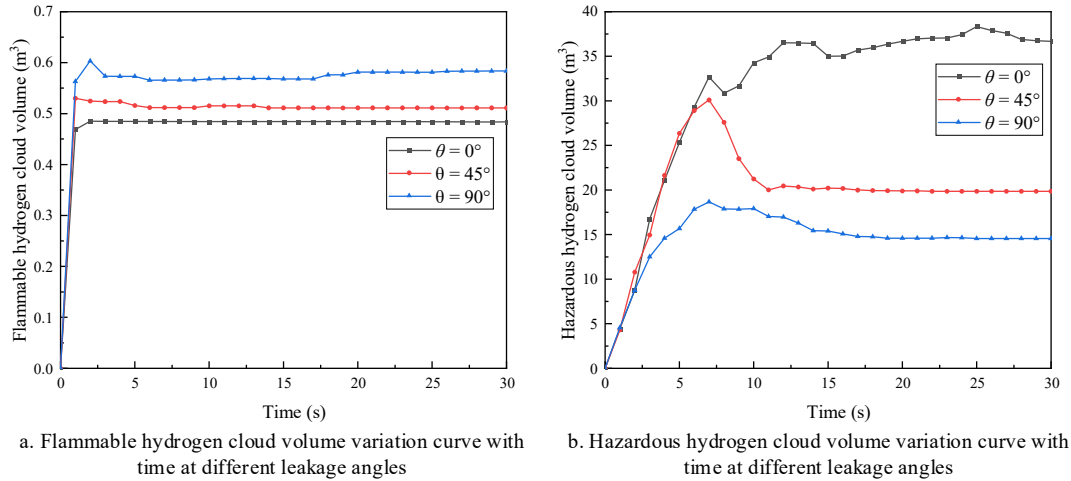


Figure 8. Flammable and hazardous hydrogen cloud volumes variation curve with time at different leakage angles

When the leakage angle $\theta=45^\circ$, the hydrogen jet was inclined to contact with the roof. The hydrogen jet diffused in the negative direction of the Y-axis under the guide effect of the roof. As shown in Figure 6 h, the hydrogen diffused along the underside of the roof showed a significant accumulation when the air obstructed it. Due to the obstacle of the roof, the accumulated hydrogen could not be discharged in time and could only spread in all directions along the horizontal. The hazardous hydrogen cloud's volume kept increasing and peaked at about $t=7$ s. Later, with horizontal momentum, the accumulated hydrogen gradually spread to the roof's edge and then into the atmosphere. The volume of the hazardous hydrogen cloud decreased significantly and reached stability at about $t=11$ s, as shown in Figure 8 b.

When the leakage angle $\theta=90^\circ$, the hydrogen jet hits the roof vertically. Since the roof was close to the leakage hole, it affected the jet's main body. At $t=3$ s, a temporary peak of the flammable hydrogen cloud volume occurred. Because the leakage hole was close to the roof's edge, the accumulated hydrogen was quickly dissipated in the atmosphere, so the volume of the flammable hydrogen cloud decreased rapidly and remained stable. Since the hydrogen jet was in vertical contact with the roof, the vertical momentum was converted into horizontal momentum under the obstacle and redirection effect of the roof, and there was a great decay of momentum. Compared with Figure 6 h, m, the vortex formed at the end of the jet was smaller for the leakage angle $\theta=90^\circ$, and the hazardous hydrogen cloud volume decreased from the peak to the steady state took longer. Compared with Figure 8 b, the volume of accumulated hydrogen was less for the leakage angle $\theta=90^\circ$, and the time to reduce the volume of the hazardous hydrogen cloud from peak to steady state was longer.

4.0 CONCLUSIONS

The leakage angles strongly influenced the diffusion of hydrogen leakage. This influence was mainly reflected in the obstructing effect of the obstacle on the hydrogen jet. When the obstacle was far from the leakage hole, the volume of the flammable hydrogen cloud did not increase. However, even if the obstacle was far away, it significantly hindered the diffusion of the thin hydrogen (1% to 4%). The hydrogen's momentum in the jet's outer layer was already reduced abruptly after being blocked by the air. If obstacles were in the way at this time, it would further reduce its momentum. Hydrogen would easily accumulate near the obstacle, thus forming a large volume of hazardous hydrogen cloud. When the obstacle was close to the leakage hole, it would directly affect the jet's main body. The volume of the flammable hydrogen cloud would increase when the obstacle blocks the hydrogen jet. However, it would not affect the diffusion of thin hydrogen with low momentum. Therefore, the effect on the volume of the hazardous hydrogen cloud was small.

ACKNOWLEDGMENTS

This work is Supported by National Key R&D Program of China (No: 2021YFB2601603).

REFERENCES.

1. Lebrouhi B E, Djoupo J J, Lamrani B, et al., Global hydrogen development-A technological and geopolitical overview. *International Journal of Hydrogen Energy*, **47**, No. 11, 2022, pp. 7016-7048.
2. Shen X, Xiu G, and Wu S. Experimental study on the explosion characteristics of methane/air mixtures with hydrogen addition. *Applied Thermal Engineering*, **120**, 2017, pp. 741-747.
3. Pang L, Wang C, Han M, et al., A study on the characteristics of the deflagration of hydrogen-air mixture under the effect of a mesh aluminum alloy. *Journal of Hazardous Materials*, **299**, 2015, pp. 174-180.
4. Shen X, Wang Q, Xiao H, et al., Experimental study on the characteristic stages of premixed hydrogen-air flame propagation in a horizontal rectangular closed duct. *International journal of hydrogen energy*, **37**, No. 16, 2012, pp. 12028-12038.
5. Yang F, Wang T, Deng X, et al., Review on hydrogen safety issues: Incident statistics, hydrogen diffusion, and detonation process. *International journal of hydrogen energy*, **46**, No. 61, 2021, pp. 31467-31488.
6. Sakamoto J, Sato R, Nakayama J, et al., Leakage-type-based analysis of accidents involving hydrogen fueling stations in Japan and USA. *International journal of hydrogen energy*, **41**, No. 46, 2016, pp. 21564-21570.
7. Birch A D, Hughes D J, and Swaffield F., Velocity decay of high pressure jets. *Combustion science and technology*, **52**, No. 1-3, 1987, pp. 161-171.
8. Li X, Christopher D M, Hecht E S, et al., Comparison of two-layer model for high pressure hydrogen jets with notional nozzle model predictions and experimental data, 6th International Conference on Hydrogen Safety, 19-21 October 2015, Yokohama, Japan.
9. Han S H, Chang D, and Kim J S., Experimental investigation of highly pressurized hydrogen release through a small hole. *International journal of hydrogen energy*, **39**, No. 17, 2014, pp. 9552-9561.
10. Birch A D, Brown D R, Dodson M G, et al., The structure and concentration decay of high pressure jets of natural gas. *Combustion Science and technology*, **36**, No. 5-6, 1984, pp. 249-261.
11. Ewan B, and Moodie K., Structure and velocity measurements in underexpanded jets. *Combustion science and technology*, **45**, No. 5-6, 1986, pp. 275-288.
12. Yüceil K B, and Ötügen M V., Scaling parameters for underexpanded supersonic jets. *Physics of Fluids*, **14**, No. 12, 2002, pp. 4206-4215.
13. Schefer R W, Houf W G, Williams T C, et al., Characterization of high-pressure, underexpanded hydrogen-jet flames. *International journal of hydrogen energy*, **32**, No. 12, 2007, pp. 2081-2093.
14. Molkov V, Makarov D, and Bragin M., Physics and modelling of underexpanded jets and hydrogen dispersion in atmosphere, *Physics of Extreme States of Matter-2009*, Russian Academy of Sciences, 2009, p. 146-149.
15. Crowl D A, and Louvar J F. *Chemical Process Safety: Fundamentals with Applications*(2nd Edition), Prentice Hall, New Jersey, 2002, p. 130.
16. Lv H, Shen Y, Zheng T, et al., Numerical study of hydrogen leakage, diffusion, and combustion in an outdoor parking space under different parking configurations. *Renewable and Sustainable Energy Reviews*, **173**, 2023, pp. 113093.
17. Hussein H, Brennan S, and Molkov V., Dispersion of hydrogen release in a naturally ventilated covered car park. *International Journal of Hydrogen Energy*, **45**, No. 43, 2020, pp. 23882-23897.